DYNAMIC GSCA (GENERALIZED STRUCTURED COMPONENT ANALYSIS) WITH APPLICATIONS TO THE ANALYSIS OF EFFECTIVE CONNECTIVITY IN FUNCTIONAL NEUROIMAGING DATA

Kwanghee Jung[1,2], Yoshio Takane[1], Heungsun Hwang[1], and Todd S. Woodward[2]

1. mcgill university

2. university of british columbia

Correspondence regarding this article should be sent to Kwanghee Jung, Department of Psychiatry, University of British Columbia, BC Mental Health and Addictions Research Institute in Child and Family Research Institute Building, Room A3-112, 938 West 28th Avenue, Vancouver, BC V5Z 4H4, Canada.
E-Mail: kwanghee.jung@ubc.ca
Phone: 604-323-2000 x3068
Fax: 604-875-3871

Dynamic GSCA (Generalized Structured Component Analysis) with applications to the analysis of effective connectivity in functional neuroimaging data

Abstract

We propose a new method of structural equation modeling (SEM) for longitudinal and time series data, named Dynamic GSCA (Generalized Structured Component Analysis). The proposed method extends the original GSCA by incorporating a multivariate autoregressive model to account for the dynamic nature of data taken over time. Dynamic GSCA also incorporates direct and modulating effects of input variables on specific latent variables and on connections between latent variables, respectively. An alternating least square (ALS) algorithm is developed for parameter estimation. An improved bootstrap method called a modified moving block bootstrap method is used to assess reliability of parameter estimates, which deals with time dependence between consecutive observations effectively. We analyze synthetic and real data to illustrate the feasibility of the proposed method.

Key words:

Generalized structured component analysis (GSCA), Structural equation modeling (SEM), Longitudinal and time series data, Alternating least squares (ALS) algorithm, A modified moving block bootstrap method, Functional neuroimaging, Effective connectivity.

1. Introduction

Hwang and Takane (2004) recently proposed Generalized Structured Component Analysis (GSCA) as a viable alternative to two conventional approaches to structural equation modeling (SEM): covariance structure analysis (CSA; Jöreskog, 1970) and partial least squares (PLS; Wold, 1973). Since their original work, GSCA has been extended and generalized to improve its data-analytic capability and applicability, e.g., dealing with cluster-level respondent heterogeneity (Hwang, DeSarbo, and Takane, 2007a), multilevel modeling (Hwang, Takane, and Malhotra, 2007b), and modulating effects of latent variables (Hwang, Ho, and Lee, 2010).

In this paper, we propose a new method of structural equation modeling for longitudinal and time series data, named Dynamic GSCA. Dynamic GSCA is a component-based method which combines the original GSCA and a multivariate autoregressive model in a unified framework to account for dynamic nature of data taken over time. Indeed, Dynamic GSCA is a comprehensive structural equation model, which is able to handle temporally correlated data (i.e., time-dependent samples), as well as independently sampled data. In addition, Dynamic GSCA incorporates direct and modulating effects of input variables on specific latent variables and on the connections between latent variables, respectively. As such, Dynamic GSCA is capable of dealing with more complex structural model than the conventional methods of SEM.

Dynamic GSCA is a general statistical method in that it is applicable for any field of study dealing with longitudinal and time series data. In this paper, however, we mainly focus on applications of the proposed method to the analysis of effective connectivity in functional neuroimaging data, which refers to a class of analysis methods that quantify the influence that one neural system exerts on another (Friston, 1994). This is intended to highlight its flexibility in model specification by handling complex brain connectivity. It might also substantiate its practical usefulness in a rapidly emerging field of science, human brain research.

To place effective connectivity modeling in perspective, we briefly introduce a typical fMRI study (Huettel, Song, and McCarthy, 2004). fMRI records changes in blood oxygenation over scans (also called time points) while an individual is presented with stimuli or asked to perform a task. The measures are called blood-oxygen level dependent (BOLD) signals. The basic element of spatial measurement in fMRI is referred to as a voxel (i.e., a three dimensional volume element), and a region of interest (ROI) consisting of a certain number of voxels is commonly used as a unit of analysis when modelling effective connectivity. That is, a number of specific brain regions are selected based on a hypothesis about their importance in completing a task, and then their directional relationships are modeled and tested, providing a statistical test of effective connectivity.

In sum, we demonstrate that the newly proposed Dynamic GSCA is appropriate for multivariate time series data, with applications to modelling effective connectivity in functional neuroimaging data, where the data matrix contains repeated measures across time points in the rows, and variables (i.e., voxels) in the columns. In the Dynamic GSCA model, BOLD signals in the voxels in a given ROI correspond to observed variables/indicators, and ROIs correspond to latent variables/constructs, indicating representative activity in the brain regions inferred from BOLD signals in voxels in the brain areas of interest.

This paper is organized as follows. In the next section (section 2), we discuss Dynamic GSCA in detail. We present the model for Dynamic GSCA (secition 2.1) and the estimation of model parameters (secition 2.2). We then discuss the GOF (Goodness of Fit) indices (secition 2.3) and a special bootstrap method for assessing the reliability of parameter estimates (secition 2.4). In section 3, we investigate performance of Dynamic GSCA in parameter recovery through Monte-Carlo simulation studies. In section 4, we illustrate the empirical validity of Dynamic GSCA with real examples. In the final section (section 5), we summarize previous sections and discuss further prospects for Dynamic GSCA.

2. Dynamic GSCA

2.1 The Model

Dynamic GSCA consists of two submodels; measurement and structural models. The measurement model specifies hypothesized relationships between observed variables and latent variables. This part of the Dynamic GSCA model remains essentially the same as in the original GSCA model (Hwang and Takane, 2004). The structural model, on the other hand, specifies hypothesized relationships among latent variables. This part of the Dynamic GSCA model has many new features to deal with the dynamic nature of time series data and accommodate input variables such as experimental stimuli in brain imaging studies, which results in more complicated structural models. Specifically, Dynamic GSCA has a mechanism for examining relationships between latent variables involving different time points (called time lagged effects) by incorporating a multivariate autoregressive model. In addition, Dynamic GSCA is able to investigate direct and modulating effects of input variables on specific latent variables and on connections between latent variables, respectively.

We begin with the measurement model. Let $\mathbf{Z}_i$ $(i = 1, \cdots, p)$ denote a T by v_i matrix of observations, where i indexes a latent variable, T indicates the number of time points, v_i the number of observed variables for latent variable i, and p the total number of latent variables. The matrix $\mathbf{Z}_i$ is assumed to be columnwise standardized. In Dynamic GSCA, a latent variable, $\boldsymbol{\gamma}_i$, is defined as an exact linear combination of the observed variables, and

it is scaled to have unit variance. Let $\mathbf{w}_i$ denote a v_i by 1 vector of component weights. Then,

$$\boldsymbol{\gamma}_i = \mathbf{Z}_i \mathbf{w}_i. \tag{1}$$

The measurement model specifies the relationship between the observed variables $\mathbf{Z}_i$ and the latent variable $\boldsymbol{\gamma}_i$. Let $\mathbf{c}_i$ denote the vector of weights applied to $\boldsymbol{\gamma}_i$ to best approximate $\mathbf{Z}_i$. Then, the measurement model for latent variable i is stated as

$$\begin{aligned} \mathbf{Z}_i &= \boldsymbol{\gamma}_i \mathbf{c}_i' + \mathbf{E}_i \\ &= \mathbf{Z}_i \mathbf{w}_i \mathbf{c}_i' + \mathbf{E}_i, \end{aligned} \tag{2}$$

where $\mathbf{E}_i$ is a T by v_i matrix of disturbance terms. Note that $\mathbf{Z}_i$ and $\boldsymbol{\gamma}_i$ are assumed to be standardized, and thus the weight vectors $\mathbf{w}_i$ and $\mathbf{c}_i$ are scaled accordingly.

For later use, it is convenient to rewrite (1) and (2) for $i = 1, \cdots, p$ as single equations. Define a row block matrix $\mathbf{Z}$ by

$$\mathbf{Z} = [\mathbf{Z}_1, \mathbf{Z}_2, \cdots, \mathbf{Z}_p]. \tag{3}$$

The total number of columns in $\mathbf{Z}$ is denoted by $V = \sum_{i=1}^{p} v_i$. Also, define a block diagonal matrix $\mathbf{D}_W$ with $\mathbf{w}_i$ as the ith diagonal block,

$$\mathbf{D}_W = \text{bdiag}([\mathbf{w}_1, \mathbf{w}_2 \cdots, \mathbf{w}_p]) = \begin{bmatrix} \mathbf{w}_1 & \mathbf{0} & \cdots & \mathbf{0} \\ \mathbf{0} & \mathbf{w}_2 & \cdots & \mathbf{0} \\ \vdots & \vdots & \ddots & \vdots \\ \mathbf{0} & \mathbf{0} & \cdots & \mathbf{w}_p \end{bmatrix} \tag{4}$$

(the operator bdiag forms a block diagonal matrix with vectors (matrices) in its argument as diagonal blocks), a similar block diagonal matrix with $\mathbf{c}_i$ as the ith diagonal block,

$$\mathbf{D}_C = \text{bdiag}([\mathbf{c}_1, \mathbf{c}_2, \cdots, \mathbf{c}_p]) = \begin{bmatrix} \mathbf{c}_1 & \mathbf{0} & \cdots & \mathbf{0} \\ \mathbf{0} & \mathbf{c}_2 & \cdots & \mathbf{0} \\ \vdots & \vdots & \ddots & \vdots \\ \mathbf{0} & \mathbf{0} & \cdots & \mathbf{c}_p \end{bmatrix}, \tag{5}$$

and a row block matrix with $\boldsymbol{\gamma}_i$ as the ith column vector,

$$\boldsymbol{\Gamma} = [\boldsymbol{\gamma}_1, \boldsymbol{\gamma}_2, \cdots, \boldsymbol{\gamma}_p]. \tag{6}$$

Then, (1) and (2) can be collectively written as

$$\boldsymbol{\Gamma} = \mathbf{Z}\mathbf{D}_W, \tag{7}$$

and

$$\mathbf{Z} = \mathbf{\Gamma}\mathbf{D}_C' + \mathbf{E}_M = \mathbf{Z}\mathbf{D}_W\mathbf{D}_C' + \mathbf{E}_M, \tag{8}$$

where

$$\mathbf{E}_M = [\mathbf{E}_1, \mathbf{E}_2, \cdots, \mathbf{E}_p]. \tag{9}$$

A necessary and sufficient condition for identification has been discussed by Kiers and Takane (1993) and Takane, Kiers, and de Leeuw (1995) for identifiability of a model similar to the above. Kiers and Takane's (1993) theorem, in particular, stipulates that $\boldsymbol{\gamma}_i (i = 1, \cdots, p)$ is disjoint with $\mathbf{Z}_j$ for all $j \neq i$. Their $\mathbf{A}$ corresponds with our $\mathbf{\Gamma}$, $\mathbf{G}_i$ with $\mathbf{Z}_i$, and the theorem almost literally applies to our situation. This condition can be easily checked after the analysis by Dynamic GSCA is conducted. Kiers and Takane (1993) also provide a sufficient condition for identification that can be checked before the analysis is made. This condition stipulates that Z has full column rank, which we assume in this paper. It is not at all difficult to satisfy this condition in most practical situations, and indeed they are satisfied in all examples we discuss in this paper.

Next, we specify the structural model, for which several more matrices have to be introduced. Let $\mathbf{u}_j$ represent the T-component vector of the jth input variable. It is assumed that each $\mathbf{u}_j$ is *a priori* standardized. (An example of an input variable vector is given in Figure 2.) It is assumed that in the general case there are k such vectors, which we denote collectively by the row block matrix $\mathbf{U} = [\mathbf{u}_1, \mathbf{u}_2, \cdots, \mathbf{u}_k]$. Let $\text{diag}(\mathbf{u}_j)$ be the diagonal matrix with elements of $\mathbf{u}_j$ as its diagonal elements. As we will see shortly, this diagonal matrix plays an important role in defining interaction effects between input variables and latent variables.

Shift matrices are now introduced to capture time lagged effects. Here, we adopt the strategy that a series of shift matrices represent both contemporaneous and lagged effects. Note that contemporaneous effects denote concurrent relations between latent variables at the same time point as in the conventional methods of SEM. Specifically, the shift matrix with time lag 0 ($\mathbf{S}_0 = \mathbf{I}_T$, where $\mathbf{I}_T$ is the identity matrix of order T) represents contemporaneous effects, while $\mathbf{S}_\ell$ ($\ell = 1, \cdots, q$) represents time lagged effects among latent variables. The subscript ℓ indexes the order of lags. The matrix $\mathbf{S}_1$, for example, represents the effect of time $t-1$ on time t. This matrix looks like:

$$\mathbf{S}_1 = \begin{bmatrix} 0 & 0 & \cdots & 0 & 0 \\ 1 & 0 & \cdots & 0 & 0 \\ 0 & 1 & \cdots & 0 & 0 \\ \vdots & \vdots & \ddots & \vdots & \vdots \\ 0 & 0 & \cdots & 1 & 0 \end{bmatrix}. \tag{10}$$

The matrix above is obtained from $\mathbf{S}_0$ by down-shifting the first $T-1$ rows of $\mathbf{S}_0$ into row 2 through row T of $\mathbf{S}_1$ and by filling the first row by a zero vector. In general, the shift matrix $\mathbf{S}_\ell = [s_{ij}^{(\ell)}]$ of lag ℓ ($\ell = 0, \cdots, q$) is defined by

$$s_{ij}^{(\ell)} = \begin{cases} 1 & \text{if } i \geq \ell + 1 \text{ and } j = i - \ell, \\ 0 & \text{otherwise.} \end{cases} \tag{11}$$

Premultiplying $\mathbf{\Gamma}$ by $\mathbf{S}_\ell$ shifts down the rows of $\mathbf{\Gamma}$ by ℓ rows and defines the matrix of the effect of latent variables at time $t-\ell$ on time t. Note that the shift matrices $\mathbf{S}_\ell$ (except $\mathbf{S}_0$) are generally singular.

The generic structural model of Dynamic GSCA can now be stated as

$$\mathbf{\Gamma} = \sum_{\ell=0}^{q} \mathbf{S}_\ell \mathbf{\Gamma} \mathbf{A}_\ell' + \sum_{\ell=0}^{q} \mathbf{S}_\ell \mathbf{U} \mathbf{D}_\ell' + \sum_{\ell=0}^{q} \sum_{j=1}^{k} \mathbf{S}_\ell \text{diag}(\mathbf{u}_j) \mathbf{\Gamma} \mathbf{M}_{\ell j}' + \mathbf{E}_S, \tag{12}$$

where the $\mathbf{A}_\ell$ are square matrices of order p of path coefficients for connections between latent variables of varying lags, the $\mathbf{D}_\ell$ are p by k matrices of path coefficients for the direct effects of input variables on latent variables, the $\mathbf{M}_{\ell j}$ are square matrices of order p of path coefficients for modulating effects of input variables on connections between latent variables, and $\mathbf{E}_S$ represents the matrix of prediction errors. These matrices typically have many prescribed zero elements representing our hypothesis that certain effects are 0. Free elements in the matrices, on the other hand, represent the hypothesis that the corresponding effects are nonzero and are to be estimated from data. The first term in (12) thus represents the contemporaneous and lagged effects between latent variables, the second term direct effects of input variables on latent variables, and the third term the modulating effects of input variables on connections between latent variables. Note that (12) reduces to the structural model of the original GSCA when there is only the first term and $q = 0$.

It is difficult to state a general identification condition for the structural model written in the form of (12) with unknown patterns of 0's in the parameter matrices. A simple and directly verifiable condition will be given right after (32).

***** Insert Figure 1 about here. *****

For illustration, an example of a path diagram is displayed in Figure 1, in which we assume that there are three latent variables ($\boldsymbol{\gamma}_1, \boldsymbol{\gamma}_2, \boldsymbol{\gamma}_3$) and three input variables ($\mathbf{u}_1, \mathbf{u}_2, \mathbf{u}_3$). In the hypothesized model, we assume that three latent variables are fully and reciprocally (bidirectionally) connected. Solid arrows indicate contemporaneous effects between latent variables. Path coefficients for these effects are denoted by a_1 through a_6. We also assume that there are autoregressive effects of lag 1 of latent variables on

themselves. Dashed arrows indicate the time lagged effects. The path coefficients associated with the autoregressive effects are denoted by a_7 through a_9 in Figure 1. Figure 1 also indicates that there were three input variable effects. We hypothetically assume that 1) the first input variable ($\mathbf{u}_1$) has a direct effect on $\boldsymbol{\gamma}_1$ (the path coefficient denoted as d_1), 2) the second input variable ($\mathbf{u}_2$) modulates the connection from $\boldsymbol{\gamma}_1$ to $\boldsymbol{\gamma}_2$ (the path coefficient denoted as m_1), and 3) the third input variable ($\mathbf{u}_3$) modulates the connection from $\boldsymbol{\gamma}_3$ to $\boldsymbol{\gamma}_1$ (the path coefficint denoted as m_2). The modulation effect here means that connectivity between latent variables is temporarily enhanced or reduced as a result of an input variable effect. The model in this diagram can be written as

$$\boldsymbol{\Gamma} = \boldsymbol{\Gamma}\mathbf{A}_0' + \mathbf{S}_1\boldsymbol{\Gamma}\mathbf{A}_1' + \mathbf{u}_1\mathbf{d}_{01}' + \text{diag}(\mathbf{u}_2)\boldsymbol{\Gamma}\mathbf{M}_{02}' + \text{diag}(\mathbf{u}_3)\boldsymbol{\Gamma}\mathbf{M}_{03}' + \mathbf{E}_S, \tag{13}$$

where

$$\mathbf{A}_0' = \begin{bmatrix} 0 & a_3 & a_5 \\ a_1 & 0 & a_6 \\ a_2 & a_4 & 0 \end{bmatrix}, \tag{14}$$

$$\mathbf{A}_1' = \begin{bmatrix} a_7 & 0 & 0 \\ 0 & a_8 & 0 \\ 0 & 0 & a_9 \end{bmatrix}, \tag{15}$$

$$\mathbf{d}_{01}' = (d_1, 0, 0), \tag{16}$$

$$\mathbf{M}_{02}' = \begin{bmatrix} 0 & m_1 & 0 \\ 0 & 0 & 0 \\ 0 & 0 & 0 \end{bmatrix}, \tag{17}$$

and

$$\mathbf{M}_{03}' = \begin{bmatrix} 0 & 0 & 0 \\ 0 & 0 & 0 \\ 0 & m_2 & 0 \end{bmatrix}. \tag{18}$$

Note that $\mathbf{d}_{01}'$ denotes the first row vector of $\mathbf{D}_0'$. In general, the rows of $\mathbf{A}_\ell'$ and $\mathbf{M}_{\ell j}'$ represent latent variables exerting influence, whereas the columns represent latent variables being influenced. The rows of $\mathbf{D}_j'$, on the other hand, represent input variables exerting influence on latent variables corresponding to the columns of $\mathbf{D}_j'$.

2.2 Parameter Estimation

In the Dynamic GSCA model, a least squares (LS) criterion is used for parameter estimation. Specifically,

$$\phi = \text{SS}(\mathbf{E}) = \text{tr}(\mathbf{E}'\mathbf{E}) \tag{19}$$

is minimized with respect to model parameters, where $\mathbf{E} = [\mathbf{E}_M, \mathbf{E}_S]$. We use an iterative algorithm called an ALS (Alternating Least Squares; e.g., de Leeuw, Young, and Takane, 1976) algorithm to find LS estimates of parameters that minimize (19). The ALS algorithm is particularly attractive in the present context because Dynamic GSCA has two natural subsets of parameters; $\mathbf{w}_i$'s that define latent variables and all other parameters (path coefficients; $\mathbf{c}_i$'s, $\mathbf{A}_\ell$'s, $\mathbf{D}_\ell$'s and $\mathbf{M}_{\ell j}$'s). The proposed ALS algorithm thus consists of two major steps:

Step I. Update $\mathbf{c}_i$'s, $\mathbf{A}_\ell$'s, $\mathbf{D}_\ell$'s, and $\mathbf{M}_{\ell j}$'s with $\mathbf{w}_i$'s being fixed.
Step II. Update $\mathbf{w}_i$'s while $\mathbf{c}_i$'s, $\mathbf{A}_\ell$'s, $\mathbf{D}_\ell$'s, and $\mathbf{M}_{\ell j}$'s are fixed.

In developing updating formula, it is helpful to "vectorize" some of the quantities. The following operations are useful for this purpose: The vec operator strings out column vectors of a matrix in its argument to form a tall supervecctor. A Kronecker product between two matrices is denoted $\mathbf{C} = \mathbf{A} \otimes \mathbf{B}$ and defined as $\mathbf{C} = [a_{ij}\mathbf{B}]$, where $\mathbf{A} = [a_{ij}]$. The following formula is commonly used for the vec of a triple matrix product $\text{vec}(\mathbf{ABC}) = (\mathbf{C}' \otimes \mathbf{A})\text{vec}(\mathbf{B}) = (\mathbf{I} \otimes \mathbf{AB})\text{vec}(\mathbf{C})$. Detailed accounts of these as well as other useful operations can be found in Harville (1997).

2.2.1 Updating path coefficients ($\mathbf{c}_i$'s, $\mathbf{A}_\ell$'s, $\mathbf{D}_\ell$'s and $\mathbf{M}_{\ell j}$'s)

The error vector $\mathbf{e}_M = \text{vec}(\mathbf{E}_M)$ for the measurement model (8) can be written as

$$\mathbf{e}_M = \mathbf{z} - (\mathbf{I}_V \otimes \mathbf{D}_Z\mathbf{w})\mathbf{c}, \tag{20}$$

where $\mathbf{z} = \text{vec}(\mathbf{Z})$,

$$\mathbf{D}_Z = \text{bdiag}(\mathbf{Z}) = \begin{bmatrix} \mathbf{Z}_1 & \mathbf{O} & \cdots & \mathbf{O} \\ \mathbf{O} & \mathbf{Z}_2 & \cdots & \mathbf{O} \\ \vdots & \vdots & \ddots & \vdots \\ \mathbf{O} & \mathbf{O} & \cdots & \mathbf{Z}_p \end{bmatrix}, \tag{21}$$

$$\mathbf{w} = \begin{pmatrix} \mathbf{w}_1 \\ \mathbf{w}_2 \\ \vdots \\ \mathbf{w}_p \end{pmatrix} = \mathbf{D}_W \mathbf{1}_p, \tag{22}$$

and $\mathbf{c} = \mathbf{D}_C \mathbf{1}_p$, where $\mathbf{1}_p$ is the p-component vector of ones. The error vector $\mathbf{e}_S = \text{vec}(\mathbf{E}_S)$ for the structural model (12), on the other hand, can be written as

$$\mathbf{e}_S = \boldsymbol{\gamma} - \mathbf{X}^* \mathbf{h}^*, \tag{23}$$

where $\boldsymbol{\gamma} = \text{vec}(\boldsymbol{\Gamma})$,

$$\mathbf{h}^* = \begin{pmatrix} \text{vec}([\mathbf{A}_0', \cdots, \mathbf{A}_q']) \\ \text{vec}([\mathbf{D}_0', \cdots, \mathbf{D}_q']) \\ \text{vec}([\mathbf{M}_{01}', \cdots, \mathbf{M}_{qk}']) \end{pmatrix}, \tag{24}$$

and $\mathbf{X}^* = [\mathbf{X}_1^*, \mathbf{X}_2^*, \mathbf{X}_3^*]$ with

$$\mathbf{X}_1^* = [\mathbf{I}_p \otimes \mathbf{S}_0 \boldsymbol{\Gamma}, \cdots, \mathbf{I}_p \otimes \mathbf{S}_q \boldsymbol{\Gamma}], \tag{25}$$

$$\mathbf{X}_2^* = [\mathbf{I}_p \otimes \mathbf{S}_0 \mathbf{U}, \cdots, \mathbf{I}_p \otimes \mathbf{S}_q \mathbf{U}], \tag{26}$$

and

$$\mathbf{X}_3^* = [\mathbf{I}_p \otimes \mathbf{S}_0 \text{diag}(\mathbf{u}_1) \boldsymbol{\Gamma}, \cdots, \mathbf{I}_p \otimes \mathbf{S}_q \text{diag}(\mathbf{u}_k) \boldsymbol{\Gamma}]. \tag{27}$$

The vector $\mathbf{h}^*$ has many 0 elements. Let $\tilde{\mathbf{h}}$ denote the vector formed from $\mathbf{h}^*$ by eliminating all of its 0 elements, and let $\tilde{\mathbf{X}}$ denote the matrix formed from $\mathbf{X}^*$ by eliminating all the corresponding columns of $\mathbf{X}^*$. Then, (20) and (23) can be collectively written as

$$\mathbf{e} = \begin{pmatrix} \mathbf{e}_M \\ \mathbf{e}_S \end{pmatrix} = \mathbf{f} - \mathbf{X}\mathbf{h}, \tag{28}$$

where

$$\mathbf{f} = \begin{pmatrix} \mathbf{z} \\ \boldsymbol{\gamma} \end{pmatrix}, \tag{29}$$

$$\mathbf{X} = \text{bdiag}([\mathbf{I}_V \otimes \mathbf{D}_Z \mathbf{w}, \tilde{\mathbf{X}}]), \tag{30}$$

and

$$\mathbf{h} = \begin{pmatrix} \mathbf{c} \\ \tilde{\mathbf{h}} \end{pmatrix}. \tag{31}$$

Thus, the update of $\mathbf{h}$ (path coefficients; $\mathbf{c}_i$'s, $\mathbf{A}_\ell$'s, $\mathbf{D}_\ell$'s and $\mathbf{M}_{\ell j}$'s) that minimizes $\mathbf{e}'\mathbf{e}$ is found by

$$\hat{\mathbf{h}} = (\mathbf{X}'\mathbf{X})^{-1}\mathbf{X}'\mathbf{f}. \tag{32}$$

Note that in (32) we assume that X has full column rank, which ensures uniqueness of $\hat{\mathbf{h}}$.

2.2.2 Updating $\mathbf{w}_i$*'s*

The measurement model (8) can be also rewritten as

$$\begin{aligned}\mathbf{e}_M &= \mathbf{z} - \begin{bmatrix} \mathbf{c}_1 \otimes \mathbf{Z}_1 & \mathbf{O} & \cdots & \mathbf{O} \\ \mathbf{O} & \mathbf{c}_2 \otimes \mathbf{Z}_2 & \cdots & \mathbf{O} \\ \vdots & \vdots & \ddots & \vdots \\ \mathbf{O} & \mathbf{O} & \cdots & \mathbf{c}_p \otimes \mathbf{Z}_p \end{bmatrix} \mathbf{w} \\ &= \mathbf{z} - (\mathbf{D}_C \otimes \mathbf{D}_Z)\mathbf{w}. \end{aligned} \tag{33}$$

Similarly, the structural model (12) can be rewritten as

$$\begin{aligned}\mathbf{e}_S = &-\mathrm{vec}(\sum_{\ell=0}^{q} \mathbf{S}_\ell \mathbf{U}\mathbf{D}_\ell') \\ &+ \boldsymbol{\gamma} - \sum_{\ell=0}^{q}(\mathbf{A}_\ell \otimes \mathbf{S}_\ell)\boldsymbol{\gamma} - \sum_{\ell=0}^{q}\sum_{j=1}^{k}(\mathbf{M}_{\ell j} \otimes \mathbf{S}_\ell \mathrm{diag}(\mathbf{u}_j))\boldsymbol{\gamma}, \end{aligned} \tag{34}$$

or by replacing $\boldsymbol{\gamma}$ by $\mathbf{D}_Z\mathbf{w}$,

$$\begin{aligned}\mathbf{e}_S = &-\mathrm{vec}(\sum_{\ell=0}^{q} \mathbf{S}_\ell \mathbf{U}\mathbf{D}_\ell') \\ &- \{-\mathbf{I} + \sum_{\ell=0}^{q}(\mathbf{A}_\ell \otimes \mathbf{S}_\ell) + \sum_{\ell=0}^{q}\sum_{j=1}^{k}(\mathbf{M}_{\ell j} \otimes \mathbf{S}_\ell \mathrm{diag}(\mathbf{u}_j))\}\mathbf{D}_Z\mathbf{w}. \end{aligned} \tag{35}$$

From (33) and (35) it follows that

$$\mathbf{e} = \mathbf{g} - \mathbf{Y}\mathbf{w}, \tag{36}$$

where

$$\mathbf{g} = \begin{pmatrix} \mathbf{z} \\ -\mathrm{vec}(\sum_{\ell=0}^{q} \mathbf{S}_\ell \mathbf{U}\mathbf{D}_\ell') \end{pmatrix}, \tag{37}$$

and

$$\mathbf{Y} = \begin{bmatrix} \mathbf{D}_C \otimes \mathbf{D}_Z \\ \{(-\mathbf{I} + \sum_{\ell=0}^{q}(\mathbf{A}_\ell \otimes \mathbf{S}_\ell) + \sum_{\ell=0}^{q}\sum_{j=1}^{k}(\mathbf{M}_{\ell j} \otimes \mathbf{S}_\ell \mathrm{diag}(\mathbf{u}_j))\}\mathbf{D}_Z \end{bmatrix}. \tag{38}$$

In this step, $\mathbf{e}'\mathbf{e}$ is minimized with respect to $\mathbf{w}_i$ separately and sequentially subject to the normalization restriction that

$$(1/T)\mathbf{w}_i'\mathbf{Z}_i'\mathbf{Z}_i\mathbf{w}_i = 1 \tag{39}$$

for each i. (A latent variable is scaled to have unit variance.) This implies that $\mathbf{e}'\mathbf{e}$ is minimized with respect to $\mathbf{w}_i$ sequentially ($i = 1, \cdots, p$) with other $\mathbf{w}_j$ ($j \neq i$) being fixed. Let $\mathbf{Y}_{(-i)}$ and $\mathbf{w}_{(-i)}$ pertain to the portions of $\mathbf{Y}$ and $\mathbf{w}$ unrelated to the variable set i, and let $\mathbf{Y}_i$ and $\mathbf{w}_i$ represent the portion of $\mathbf{Y}$ and $\mathbf{w}$ specifically related to i. Then, the portion of $\mathbf{g}$ unrelated to the variable set i can be written as $\mathbf{g}_{(-i)} = \mathbf{g} - \mathbf{Y}_{(-i)}\mathbf{w}_{(-i)}$, and $\mathbf{e}$ in (36) can be written as $\mathbf{e} = \mathbf{g}_{(-i)} - \mathbf{Y}_i\mathbf{w}_i$. As a result, $\mathbf{e}'\mathbf{e}$ is minimized with respect to $\mathbf{w}_i$ for a specific i subject to the normalization restriction in (39). Note that $\mathbf{Y}_i$ is assumed to have full column rank. This ensures uniqueness of the estimates of $\mathbf{w}_i$. There is a special algorithm to solve a minimization problem of this form developed by ten Berge and Nevels (1977), which we used in our program. Once $\mathbf{w}_i$ is updated, it has to be immediately put back into redefining the next $\mathbf{g}_{(-i)}$ in order to preserve the monotonic convergence property of the ALS algorithm. Thus, we update $\mathbf{w}$ in (36) using the sequentially updated $\mathbf{w}_i$'s in this step, and we calculate the sum of squares of errors ($\mathbf{e}'\mathbf{e}$) using $\mathbf{e}$ in (36).

The two steps described above are repeatedly applied until the change in $\mathbf{e}'\mathbf{e}$ from one iteration to the next gets smaller than a certain prescribed value, say 1.0E-6.

2.3 GOF Indices

In Dynamic GSCA, the overall fit of a hypothesized model is measured by predictability of the specified model, which is given by

$$\text{FIT} = 1 - \frac{\text{SS}(\mathbf{g} - \mathbf{Y}\hat{\mathbf{w}})}{\text{SS}(\mathbf{g})}, \tag{40}$$

where $\hat{\mathbf{w}}$ is the estimate of $\mathbf{w}$ at a convergence point of the ALS algorithm presented in the previous section. This fit index (FIT, Hwang and Takane, 2004) ranges from 0 to 1. The larger the FIT value, the larger the proportion of the variance in the endogenous variables explained by the model. It is inversely related to the sum of the squared residuals indicating the overall discrepancy between the model and data.

However, FIT is obviously affected by model complexity, i.e., the larger the number of parameters in the model, the larger the value of FIT we get. Hence, we use an alternative fit measure which takes into account the complexity of a fitted model. This fit measure is called adjusted FIT or AFIT (Hwang et al., 2007a), and is given by

$$\text{AFIT} = 1 - (1 - \text{FIT})\frac{n_0}{n_1}, \tag{41}$$

where $n_0 = TV$ is the degree of freedom for the null model (i.e., the model with no structural relationships among latent variables), $n_1 = TV - r$ is the degree of freedom for the model being tested, where V is the total number of observed variables, and r is the number of free parameters in the hypothesized model. The AFIT measure takes into account the number of parameters used in the model. This measure typically favors simpler models over complex models given similar explanatory power. A model that maximizes AFIT is regarded as the best model among all competing models.

2.4 A Special Bootstrap Method

In the original GSCA, a bootstrap method is used for assessing the reliability of parameter estimates, since it is impossible to obtain analytic expressions for standard errors of parameter estimates (Efron, 1982). However, the standard bootstrap method used in the original GSCA is not appropriate for time series data because it does not take into account the time order of observations, and consequently it results in incorrect standard error estimates (Lahiri, 2003). Thus, in Dynamic GSCA, a modified moving block bootstrap method is employed to deal with this problem. (For more details, see Bühlmann, 2002; Zhang and Browne, 2010).

Specifically, the modified moving block bootstrap method implemented in Dynamic GSCA can be described by the following three steps. In the first step, we break down the original data into overlapping blocks of size L (L = the order of lagged effect+1). For instance, in case of the effect of lag 1, the first block consists of $(z_1, z_2)'$, the second block $(z_2, z_3)'$, and the tth block $(z_t, z_{t+1})'$. Here, z_t is a vector of variables measured at time t. The overlapping blocks are supposed to capture the dependence among consecutive observations. In the second step, we draw blocks of observations with replacement up to the number of time points (T). As a result, we obtain $T \times L$ bootstrap samples. In the third step, we apply Dynamic GSCA to the bootstrap samples. This step, however, requires special attention, as described below.

For illustration, suppose that the model has only the first order lagged effect ($L = 2$) and that we are updating $\mathbf{h}$ in the first phase of the ALS algorithm. We create $\mathbf{X}_b$ and $\mathbf{f}_b$ (analogous to $\mathbf{X}$ and $\mathbf{f}$) from the bootstrap samples created in the previous step of the bootstrap procedure. Even rows of $\mathbf{X}_b$ and $\mathbf{f}_b$ contain the information of the first order lagged effect, whereas odd rows represent the effects of bad joints denoting the time sequences that did not exist in the original data. This can be easily demonstrated by using the following simple bootstrap sample: $(z_1, z_2, z_5, z_6)'$. The second and fourth rows of $\mathbf{X}_b$ and $\mathbf{f}_b$ consisting of $(z_1, z_2)'$ and $(z_5, z_6)'$ capture the first order time lagged effect given the data, while the third row of $\mathbf{X}_b$ and $\mathbf{f}_b$ consisting of $(z_2, z_5)'$ capture merely pseudo

time lagged effect. The first row of $\mathbf{X}_b$ and $\mathbf{f}_b$ also has nothing to do with the first time lagged effect because z_1 has no pair. Hence, we deliberately eliminate the odd rows of $\mathbf{X}_b$ and $\mathbf{f}_b$, and obtain the reduced $\mathbf{X}_b$ and $\mathbf{f}_b$, denoted by $\tilde{\mathbf{X}}_b$ and $\tilde{\mathbf{f}}_b$. Then we use $\tilde{\mathbf{X}}_b$ and $\tilde{\mathbf{f}}_b$ instead of $\mathbf{X}_b$ and $\mathbf{f}_b$, respectively, in updating $\mathbf{h}$. Essentially the same method has to be used in updating $\mathbf{w}_i$ in the second phase of the ALS algorithm.

The three steps described above are repeated for as many bootstrap samples as needed. Estimates of parameters are obtained for each bootstrap sample, and then means and variances of the estimates are calculated across the bootstrap samples to obtain standard errors of the estimates. Empirical distributions of parameter estimates derived by the bootstrap procedure may not be symmetric. In that case, it may be more practical to obtain confidence intervals based directly on the empirical distribution of the parameter estimates.

Significant tests of estimated coefficients may also be performed as a by-product of the bootstrap procedure. Specifically, the number of times bootstrap estimates "crossing" over zero is counted for a significant test (if the original estimate is positive, the number of times the bootstrap estimates turn out to be negative is counted, and vice versa). If the relative frequency (p-value) of crossovers comes to less than a prescribed α level, it is concluded that the coefficient is significantly positive (or negative). This counting method is used in Dynamic GSCA because it requires no parametric assumption such as the asymptotic normality of parameter estimates, which may not hold in practice.

Note that our model assumes that serial correlations are fully captured by the time lag effects included in the structural model. There is always a question of whether a sufficient number of the time lag effects are included in the model. In the examples of analysis of fMRI data, we always assume that the first order time lag effects are sufficient to "explain away" all the serial correlations. In the fMRI data, the time resolution is typically not very high, and thus inclusions of higher order time lag effects are not likely to be substantively important. There is also some evidence in the literature (e.g., Gates et al., 2011) that serial correlations beyond order 1 are negligible, once the first order time lag effects are taken into account.

3. Simulation Studies: Recovery of Parameters

In this section, we report two Monte Carlo studies designed to show that Dynamic GSCA works the way it is supposed to. We considered two different structural models varying in the number of latent variables (i.e., 3 and 7) and in hypothesized relationships among them. They were designated to illustrate flexibility of the proposed method in model specification. Furthermore, we also considered the number of time points (sample

sizes), and the size of random errors in both measurement and structural models as two important factors influencing the goodness of parameter recovery.

3.1 Study 1: A SEM with Three Latent Variables with Three Observed Variables per Latent Variable

In this simulation study, we employed the path diagram (structural models) as depicted in Figure 1. Recall that in Figure 1, we used a structural equation model that involved three latent variables ($\boldsymbol{\gamma}_i$, $i = 1, \cdots, 3$) and three input variables ($\mathbf{u}_j$, $j = 1, \cdots, 3$). The structural models used in this study can be stated as

$$\boldsymbol{\gamma}_1 = \boldsymbol{\gamma}_2 a_1 + \boldsymbol{\gamma}_3 a_2 + \mathbf{S}_1\boldsymbol{\gamma}_1 a_7 + \mathbf{u}_1 d_1 + \mathbf{e}_1,$$
$$\boldsymbol{\gamma}_2 = \boldsymbol{\gamma}_1 a_3 + \boldsymbol{\gamma}_3 a_4 + \mathbf{S}_1\boldsymbol{\gamma}_2 a_8 + \text{diag}(\mathbf{u}_2)\boldsymbol{\gamma}_1 m_1 + \text{diag}(\mathbf{u}_3)\boldsymbol{\gamma}_3 m_2 + \mathbf{e}_2,$$
$$\boldsymbol{\gamma}_3 = \boldsymbol{\gamma}_1 a_5 + \boldsymbol{\gamma}_2 a_6 + \mathbf{S}_1\boldsymbol{\gamma}_3 a_9 + \mathbf{e}_3,$$

where $\mathbf{S}_1$ is the shift matrix of lag 1 and $\mathbf{e}_i$'s ($i = 1, \cdots, 3$) are vectors of prediction errors. Prescribed parameter values of path coefficients in the specified model are as follows:

Coefficients	a_1	a_2	a_3	a_4	a_5	a_6	a_7	a_8	a_9	d_1	m_1	m_2
Parameters	0.5	0.2	0.3	0.4	0.4	0.3	0.4	0.2	0.4	0.2	0.4	0.3

We also specified measurement models with three observed variables for each of the three latent variables:

$$\mathbf{Z}_1 = \boldsymbol{\gamma}_1 \mathbf{c}_1' + \mathbf{E}_1,$$
$$\mathbf{Z}_2 = \boldsymbol{\gamma}_2 \mathbf{c}_2' + \mathbf{E}_2,$$
$$\mathbf{Z}_3 = \boldsymbol{\gamma}_3 \mathbf{c}_3' + \mathbf{E}_3,$$

where the component loading vectors were assumed to be $\mathbf{c}_i = (0.7, 0.8, 0.9)'$ for $i = 1, \cdots, 3$. The loadings indicate the strength of relationships between observed variables and latent variables.

The data were generated with varying numbers of time points ($T = 50$, 100, 200, and 1000). Specifically, we followed a two-step procedure to generate simulated data. In the first step, we generated latent variables ($\boldsymbol{\Gamma}$) using the given parameters. For example, (13) can be rearranged as follows,

$$\boldsymbol{\Gamma} = (\mathbf{I} - \mathbf{A}_0')^{-1}(\mathbf{S}_1\boldsymbol{\Gamma}\mathbf{A}_1' + \mathbf{u}_1\mathbf{d}_{01}' + \text{diag}(\mathbf{u}_2)\boldsymbol{\Gamma}\mathbf{M}_{02}' + \text{diag}(\mathbf{u}_3)\boldsymbol{\Gamma}\mathbf{M}_{03}' + \mathbf{E}_S). \tag{42}$$

Each row of $\boldsymbol{\Gamma}$ was generated sequentially using all other known parameters. Note that the first row vector of $\mathbf{S}_1\boldsymbol{\Gamma}$ denoting the previous latent variables was randomly sampled from a uniform distribution, and the errors in the structural models were assumed to follow a

normal distribution with zero mean and variance τ^2, where $\tau^2 = .5$, 1, or 2. Then, the latent variables ($\mathbf{\Gamma}$) were standardized. In the second step, the observed variables for each latent variable were generated using the predefined component loadings and errors, based on the measurement model, $\mathbf{Z}_i = \boldsymbol{\gamma}_i \mathbf{c}_i' + \mathbf{E}_i$. Errors in the measurement models were also assumed to follow a normal distribution with zero mean and variance σ^2, where σ^2 was varied at four levels ($\sigma^2 = 0.3$, 0.5, 0.7, or 0.9). These variances roughly correspond with the situations in which the first principal component in each latent variable accounts for 92%, 82%, 72%, and 62% of the total variance in observed variables for the latent variable.

The input variable ($\mathbf{u}_1$) is depicted in Figure 2. Input variables could be any kind of time series vectors of interest, but we here used the input vectors, simulating hemodynamic response function (HRF) in functional neuroimaging studies. Specifically, we first generated a delta function (0 = no stimulus, 1 = stimulus) with experimental stimuli presented every 15th time point starting at time 5 (in the upper panel), and then the inputs were convolved with a gamma function to model the hemodynamic response (in the bottom panel). Here, we used Statistical Parametric Mapping (SPM; Wellcome Institute of Cognitive Neurology, London, UK, http://www.fil.ion.ucl.ac.uk/spm) for the convolution. Other input variables ($\mathbf{u}_2$ and $\mathbf{u}_3$) were similarly generated with different intervals of stimulus presentation, that is, every 25th time point for $\mathbf{u}_2$ and every 35th time point for $\mathbf{u}_3$, respectively.

***** Insert Figure 2 about here. *****

As allured in the parameter estimation section (2.2), we need initial values of $\mathbf{w}_i$ in the ALS algorithm. For this, we used weights for the first principal component of $\mathbf{Z}_i$ as initial values of $\mathbf{w}_i$. Note that we have also run the ALS procedure with many random initial starts (i.e., 100 different sets) of $\mathbf{w}_i$ to see if the convergence point is the global minimum, and observed that the algorithm converged to the same minimum.

To measure the goodness of parameter recovery, we used the congruence coefficient between parameters and their estimates (Tucker, 1951) in this and subsequent simulation studies. The congruence coefficient is defined as follows: Let θ and $\hat{\theta}$ denote the vectors of the true parameters and their estimates from a single replication, respectively. Then, the congruence coefficient is given by $\theta'\hat{\theta}/(\sqrt{\theta'\theta}\sqrt{\hat{\theta}'\hat{\theta}})$. A value of the congruence coefficient greater than 0.9 is conventionally regarded as an acceptable degree of agreement (Mulaik, 1972) between parameters and the corresponding estimates.

***** Insert Table 1 about here. *****

The average congruence coefficients over 100 replications were presented in Table 1. Results for $T = 1000$ and $\tau^2 = 0.5$ have been omitted from the table because they can be

easily extrapolated from the rest of the table. We observed that the number of time points (T) and the amounts of errors (σ^2 and τ^2) in both measurement and structural models had significant influence on parameter recoveries of path coefficients ("path"). Overall, values of the congruence coefficient on path coefficients increased as the number of time points increased, and they decreased as the amounts of errors increased. However, Dynamic GSCA indeed provided reasonable recoveries (mean congruency coefficients greater than 0.9) across all conditions with a few exceptions (the number of time points was 50 and the amount of errors in measurement models was 0.7 or 0.9). Furthermore, we observed that the recovery of component loadings ("loadings") was very good and stable across conditions.

3.2 Study 2: A SEM Seven Latent Variables with Three Observed Variables per Latent Variable

The second simulation study was similar to the previous one, except that the number of latent variables involved was increased to seven, which were nearly fully connected by contemporaneous reciprocal (bidirectional) relations and by autoregressive paths. For structural models used in this study, however, there were no input variables in this example, so that both the second and third terms on the right-hand side of the generic specification given in (12) did not exist. In the first term, only the contemporaneous effects ($\ell = 0$) and the autoregressive effects of lag 1 ($\ell = 1$) were present. Path coefficients for the contemporaneous effects were set to:

$$\mathbf{A}_0' = \begin{bmatrix} 0 & -0.3 & -0.2 & 0 & 0.2 & 0.2 & 0 \\ -0.5 & 0 & -0.5 & 0 & 0.5 & 0.2 & 0.3 \\ -0.4 & -0.5 & 0 & 0 & 0.2 & 0.4 & 0 \\ 0 & -0.2 & 0 & 0 & 0.3 & -0.3 & 0.5 \\ 0.5 & 0.4 & 0.2 & 0.3 & 0 & 0.3 & -0.5 \\ 0.4 & 0.2 & 0.5 & 0 & 0.3 & 0 & 0.5 \\ 0 & 0.4 & 0 & 0.5 & -0.5 & 0.4 & 0 \end{bmatrix},$$

and those for the autoregressive effects to:

$$\mathbf{A}_1' = \text{diag}(0.4, 0.2, 0, 0.4, 0.3, 0, 0),$$

where diag indicates a diagonal matrix with elements of the vector in its argument as the diagonal elements. The diagonal elements of matrix $\mathbf{A}_0'$ were all 0. This implies there was no contemporaneous effects of latent variables on themselves. The matrix $\mathbf{A}_1'$ was diagonal, meaning that there were only the time lag effects of latent variables on themselves. Note

that there were zero off-diagonal elements in $\mathbf{A}_0'$ as well as zero diagonal elements in $\mathbf{A}_1'$. This implies that latent variables were not completely connected. However, the data generated were analyzed as if they were fully connected. That is, path coefficients assumed to be zero in the population were estimated as if they were nonzero. This was motivated by the fact that an investigator often has no clear idea about which connections really exist. Thus, he/she may fit a more comprehensive model in the hope that an analysis reveals nonsignificant connections, which may be subsequently removed from the model. The total number of path coefficients estimated in this example is 49.

The data were generated in the same manner as in study 1, except that there were three observed varibles per latent variable with a slightly different component loading vector of $\mathbf{c}_i = (0.6, 0.7, 0.8)'$ $(i = 1, \cdots, 7)$. Note that due to somewhat smaller values of the component loading used in this study the approximate percentage of variances accounted for by the first principal components tended to be smaller than in study 1 (89%, 78%, 67%, and 59%).

The average congruence coefficients were similar to those obtained in study 1. That is, the congruency coefficients on path coefficients increased as the number of time points (T) increased. They decreased as the amount of errors (σ^2) in measurement models increased. Contrary to study 1, however, the amount of errors (τ^2) in structural models did not make much difference in parameter recovery. Overall, however, Dynamic GSCA provided reasonable parameter recoveries (the average congruency coefficients are greater than 0.9 in all cases for $T = 100$ and 200). Similar to study 1, we also observed that the recovery of component loadings was fairly good and stable across conditions.

So far, all 49 parameters estimated have been treated "equally". However, among those 49 parameters, 13 parameters were assumed to be zero, while the remaining 36 parameters were assumed nonzero in generating the data. It is thus possible to investigate how many times zero parameters are judged to be significantly nonzero (α level), and how many times nonzero parameters are judged to be significantly nonzero (power) when a certain significance testing procedure is applied.

We first approximated standard errors of the estimates by calculating their standard deviations over the 100 replicated data sets in each condition. We then formed critical ratios by dividing the estimates by the corresponding standard errors. The critical ratios exceeding 2 in absolute value were judged to be significantly different from zero. The value of 2 roughly corresponds with the α level of .05 in the standard normal distribution.

Table 2 reports average powers and average α levels across all 36 parameters assumed to be nonzero (powers) and 13 parameters assumed to be zero (α levels) in the data generation. Note that the powers obviously depend on how nonzero the assumed parameter values are (the further they are away from zero, the higher is the power expected). The

average powers were calculated, however, disregarding the fact that nonzero parameters are not equally nonzero. It was hoped that this somewhat crude method was still sufficient to see general trends. The results showed that the power increased as the number of time points (T) increased, and it decreased as the amount of errors (σ^2 and τ^2) increased. It seems that overall a reasonable degree of power is achieved when the sample size is large. The average α level was nearly all zero across all conditions. This means that when the parameters are zero, it is almost never judged to be significantly different from zero. The test applied may, however, be a bit too conservative.

Finally, it should be noted that in our simulation studies, all errors were assumed to follow a normal distribution. However, this assumption may be questionable in some applications. Further simulation studies will be necessary in the future, taking into account a greater variety of conditions, such as non-normal data, correlated errors, and mis-specified models, for more thorough investigations of the performance of the proposed method.

***** Insert Table 2 about here. *****

4. Applications Dynamic GSCA to Real Functional Neuroimaging Data

In this section, we applied Dynamic GSCA to two real data sets for the purpose of demonstrating its usefulness in empirical research. In the first data set, a subject's attention to visual motion was experimentally manipulated, and its direct effect on a ROI and its modulating effect on connectivity between ROIs were investigated. The second data set involved a memory task. In this example, a relatively large number of ROIs (seven) were postulated, which were assumed to be fully connected. We examined the significance of connections by Dynamic GSCA. Recall that a ROI indicates representative activity inferred from BOLD signals in voxels in the brain areas of interest, and it is represented by a latent variable in Dynamic GSCA.

4.1 The Attention to Visual Motion Data

The first example pertains to the "attention to visual motion" data available from the SPM web site (http://www.fil.ion.ucl.ac.uk/spm/data/attention/). In the experiment, subjects performed a visual motion processing task under four different experimental conditions while undergoing fMRI. The four experimental conditions were fixation, static (non-moving dots), no attention (moving dots but no attention required), and attention. Three experimental stimuli (i.e., input variables) were created by combining the four con-

ditions: photic ($\mathbf{u}_1$, comprising all conditions with visual inputs), motion ($\mathbf{u}_2$, including all conditions with moving dots), attention ($\mathbf{u}_3$, including the only conditions with attention to moving dots). These three experimental stimuli were entered into the Dynamic GSCA model. See the three top panels of Figure 3, where the three stimulus vectors were depicted as a function of time.

***** Insert Figure 3 about here. *****

The BOLD signals for three ROIs were extracted using the SPM software: V1 (the primary visual cortex), V5 (middle temporal area), and SPC (superior parietal cortex). Specifically, all activated voxels over a threshold level corresponding to an experimental condition were first identified using SPM, and then BOLD signals for a ROI were selected with an 8mm sphere centered on the global maxima within a ROI (for more details, see Friston et al., 2007). A total of 92 BOLD signals were selected as multiple indicators for the three ROIs and used in the Dynamic GSCA model: 54 BOLD signals for V1, 24 BOLD signals for V5, and 14 BOLD signals for SPC. The 92 BOLD signals were extracted from each of 360 scans ($T = 360$) with the time interval of 3.22 seconds.

Time series of BOLD signals were presented in the bottom portions of Figure 3. The fourth, fifth, and sixth panels depict BOLD signals on a single voxel in each of the three ROIs. These were examples of the observed variables used in Dynamic GSCA. The bottom three panels indicate BOLD signals from all selected voxels within the three ROIs (superimposed on top of each other) to show how variable they are in general within the ROIs. It could be seen that although there was quite a bit of variability among the voxels, there was also some common variability across voxels within a ROI. This common variability was our main focus of analysis. It was deemed representative of neuronal activities in the ROI, and was to be captured in the form of a latent variable along with its relations to activities in other ROIs (contemporaneous effects on other ROIs), to stimulus inputs (effects of experimental stimuli), and to its previous states (autoregressive effects).

The structural model used in this analysis was the same as that depicted in Figure 1. That is, in the hypothesized model, we assumed that three ROIs were fully and reciprocally (bidirectionally) connected. We also assumed that there were autoregressive effects of lag 1 of ROIs on themselves. Furthermore, we hypothesized that 1) the experimental input "photic" ($\mathbf{u}_1$) had a direct effect on V1 ($\boldsymbol{\gamma}_1$), 2) the experimental manipulation "motion" ($\mathbf{u}_2$) modulated the connection from V1 ($\boldsymbol{\gamma}_1$) to V5 ($\boldsymbol{\gamma}_2$), and 3) the experimental manipulation "attention" ($\mathbf{u}_3$) modulated the connection from SPC ($\boldsymbol{\gamma}_3$) to V5 ($\boldsymbol{\gamma}_2$).

Dynamic GSCA was applied to fit the specified model to the data. The overall fit of the model was found to be FIT = 0.767 and AFIT = 0.766, indicating that the specified model accounted for about 77% of the total variance of all observed and latent variables.

Table 3 shows estimates of path coefficients, their standard errors, and p-values. Bootstrap standard errors were calculated based on 500 bootstrap samples using the modified moving block bootstrap method. All contemporaneous effects (a_1 through a_6) were significant at $\alpha = .05$. Only one autoregressive effect (a_7) turned out be significant, while the other two autoregressive effects (a_8 on V1 and a_9 on SPC) were not significant. The direct effect (d_1) of $\mathbf{u}_1$ on V1 was significant. However, neither of the two modulating effects of experimental stimuli were significant.

To confirm some of these effects, we displayed the time series of $\mathbf{u}_1$, the three latent variables representing the three ROIs, and interaction effects between $\mathbf{u}_2$ and V1, and $\mathbf{u}_3$ and SPC in Figure 4. At the top, there is a time series of $\mathbf{u}_1$, which looks fairly highly correlated with V1 (i.e., r=0.73). As such, this confirms the significant direct effect of $\mathbf{u}_1$ on V1. At the third and fifth pannels, there are the time series of the modulating effects of $\mathbf{u}_2$ and $\mathbf{u}_3$, which are only negligibly correlated with V5 in the fourth pannel (i.e., r= -0.10 and r=0.06, respectively). Thus, it makes intuitive sense that these modulating effects are not significant.

***** Insert Table 3 about here. *****

***** Insert Figure 4 about here. *****

In addition, the relationships between the ROIs and their respective indicators (i.e., BOLD signals) were fairly strong and homogeneous. Most component loadings were positive and higher than .80.

4.2 The Memory Data

In the second example, we again considered fully and bidirectionally connected structural models. In contrast to the first example, the number of ROIs was increased from three to seven, and no stimulus input was considered in this example. This hypothesized structural equation model was identical to that which we used in the simulation study 2. This model is a popular brain network analysis model (Smith, et al., 2010), which is also known as being difficult to fit by conventional methods of SEM based on analysis of covariance structures (e.g., Gates et al., 2011) due to computational difficulties.

In this example, we used the data collected as part of a larger study examining changes in topological patterns of large-scale functional brain networks during the performance of memory tasks (Grady et al., 2006) available at the fMRI Data Center (http://www.fmirdc.org). In the study, participants performed four encoding and two recognition tasks. The encoding tasks involved the presentation of pictures or words in

either perceptual or semantic conditions. After encoding tasks, subjects performed two recognition tasks. In each recognition condition, participants responded as to whether each stimulus was familiar or novel.

Using the data, Wang et al. (2010) found several network hubs in association cortices regions using a correlation-based network analysis. Specifically, in their analysis, the fMRI data was first parceled into 90 cortical and subcortical regions (ROIs) using an automated anatomical labeling brain atlas. Then, a representative time series with 154 data points was extracted for each ROI by averaging the BOLD signals over all voxels within the ROI. They then conducted a correlation-based network analysis to reveal alterations in topology of functional brain networks during the performance of memory tasks.

For the present analysis, we used the data extracted from one adult belonging to an older adult group (the mean age of this group was 74.4 years) during a recognition task. We adopted the network hubs of older adults in a recognition task, revealed by Wang et al. (2010), and constructed a hypothesized structural equation model. Specifically, the network hubs consisted of seven ROIs in the left-hemisphere: Insula (INS), Median cingulate and paracingulate gyri (DCG), Hippocampus (HIP), Middle occipital gyrus (MOG), Precuneus (PCUN), Thalamus (THA), and Middle temporal gyrus (MTG). The number of BOLD signals was 542 in INS, 575 in DCG, 268 in HIP, 968 in MOG, 1064 in PCUN, 305 in THA, and 1487 in MTG. There were simply too many BOLD signals to be processed for each ROI. So they were aggregated into five distinct signals for each ROI, capturing representative patterns of BOLD signals within the ROI. We calculated the centroids of clusters, which were used as indicators of ROIs in Dynamic GSCA. For the cluster analysis, the K-means algorithm in MATLAB was used (www.mathworks.com).

Dynamic GSCA was applied to fit the specified model to the data. The specified model provided FIT = 0.714 and AFIT = 0.709, indicating that it accounted for about 71% of the total variance of all observed and latent variables. Tables 4 show estimates of path coefficients, their standard errors, and p-values. Note that the diagonal portion of the table denotes the autoregressive effects of ROIs on themselves. As before, the bootstrapped standard errors were calculated based on 500 bootstrap samples using the modified moving block bootstrap method.

***** Insert Table 4 about here. *****

From the table, we observed that a majority of path coefficients were found to be significant. There were 10 nonsignificant contemporaneous effects and 3 nonsignificant autoregressive effects.

In this example, most component loadings were higher than .80 with positive signs, indicating the relationships were fairly strong and homogeneous. However, one of the com-

ponent loadings of PCUN was not significant statistically, showing a negative sign (i.e., -0.143). It suggests that we would better remove the indicator in constructing the ROI (i.e., PCUN). This result implies that we may benefit from Dynamic GSCA in defining ROIs more adequately by assessing validity and reliability of indicator variables (e.g., BOLD signals) to be included in an analysis of effective connectivity.

Summary and Discussion

In this paper, we proposed Dynamic GSCA as a new method of SEM for multivariate time series data. Dynamic GSCA extends the original GSCA by incorporating a multivariate autoregressive model to deal with the dynamic nature of data taken over time. Dynamic GSCA is capable of examining both contemporaneous and time lagged effects between latent variables, as well as direct and modulating effects of input variables on the latent variables and their connections. Using the modified moving block bootstrap method, Dynamic GSCA is also able to assess the reliability of parameter estimates despite the presence of dependencies among observations over time.

We demonstrated the usefulness of Dynamic GSCA using synthetic and real data in terms of flexibility in model specification. In the Monte Carlo studies, we reported that Dynamic GSCA was capable of recovering original parameter values with reasonable accuracy (i.e., over 90% congruence between parameters and their estimates) even in small samples, especially when the amounts of errors in measurement and structural models were small. In empirical examples, we showed that Dynamic GSCA enables researchers to specify complex reciprocal relations in the structural equation model and provide stable parameter estimates without any computational difficulties, such as improper solutions and non-convergence.

Here, we point out that there are two path-analytic SEMs without a measurement model for multivariate time series data, called the unified SEM (Kim et. al., 2007) and the extended unified SEM (Gates et al., 2011). The path-analytic SEMs have similar features to Dynamic GSCA for incorporating time lagged effects and input variable effects. In parameter estimation, as in covariance structure analysis, they use a lagged correlation matrix as input, and a maximum likelihood estimation method based on multivariate normality assumption is used.

Compared to the existing methods of SEM for multivariate time series data, Dynamic GSCA has several advantages. First, Dynamic GSCA has a single optimization criterion, including both measurement and structural models in a unified framework. As such, the previous SEMs are a special case of Dynamic GSCA in which a single indicator/observed variable is taken as a latent variable. Second, Dynamic GSCA employs an improved boot-

strap method to deal with time dependence between consecutive observations more appropriately. Thus, Dynamic GSCA may provide more accurate S.E. of parameter estimates when the data are serially correlated. Finally, Dynamic GSCA uses an alternating least squares algorithm for parameter estimation. Thus, it computationally benefits from a least squares parameter estimation method with less distributional assumptions and no model identification problems or improper solutions. On the other hand, the path-analytic SEMs are prone to have computational difficutlies in model identification and convergence of iterative algorithms as the model complexity increases (e.g., the number of latent variables and observed variables, and the number of directional paths among latent variables). Consequently, Dynamic GSCA is able to deal with more elaborate and complicated models than the existing methods.

The Dynamic GSCA model may be extended in a variety of ways to enhance its data-analytic capability and applicability. The possible enhancements include simultaneous analysis of multi-sample data, analysis of hierarchically structured data (multilevel analysis), incorporating interactions among latent variables, and an alternative minimization criterion, which we in turn elaborate below.

Dynamic GSCA is currently capable of analyzing a single sample data at a time. Here, a sample may refer to a subject. However, Dynamic GCSA can be extended to simultaneously analyze multiple-sample data. There are at least two promising possibilities. One approach is based on multi-sample (multi-group) comparison (Hwang and Takane, 2004), and the other based on multilevel analysis (Hwang et al., 2007b). In the former, the same structural model is fitted to more than one sample simultaneously with some of the path coefficients assumed equal across samples while others are assumed to vary over the samples.

The second approach deals with hierarchical structures of observed data. For instance, typical functional neuroimaging data are hierarchically structured in that their individual-level measures (e.g., BOLD signals) are grouped within higher-level units (e.g., groups/subjects/trials). In this approach, observed data are split into between-samples and within-samples data, each of which is separately modeled by SEM. This analysis allows us to investigate cross-level interactions of explanatory variables for loadings and path coefficients in different levels. Multilevel Dynamic GSCA is an extension of the original multilevel GSCA (Hwang et al., 2007b) to accommodate multivariate time series data.

Another possible extension of Dynamic GSCA involves incorporation of latent interactions. A latent (linear by linear) interaction is defined as a product of interacting latent variables (Hwang et al., 2010). This extension of Dynamic GSCA may be particulary useful for brain connectivity analysis to model changes in the magnitude of path coefficients between ROIs as a function of activities of different ROIs, thereby capturing important as-

pects of neuronal interactions. This kind of feature has been required for modeling complex neurobiological processes, including top-down modulation, learning and effects exerted by neuromodulatory transmitters (Stephan et al., 2008).

Yet another possible extension involves the minimization criterion used. So far, we implicitly assumed that all equations (in both measurement and structural models) are equally important. However, there may be hundreds of measurement equations with just a few structural equations. In such cases, criterion (19) will put a large emphasis on the measurement part, while neglecting the structural part, resulting in latent variables that are nearly equal to the principal components of observed variables. Therefore, it may make sense, in some cases, to give larger weights to the structural part to balance the contributions of the two types of submodels in the global structural equation model. This can be done by employing a weighted LS criterion instead of the unweighted LS criterion (Abdi, 2003).

We have written a MATLAB program for Dynamic GSCA to obtain the results reported in this paper. The codes of our program can be further optimized to speed up the algorithm. One promising idea is to use symbolic computations in some parts (Takane, 2009) of the program. Specifically, the equations of both measurement and structural models can be simplified as much as possible at a symbolic level, and actual numerical values are plugged in only at the final stage. As a result, final updating equations become simpler and smaller in size, and Dynamic GSCA will be able to handle more complex structural models with a larger number of observed variables.

Acknowledgements The work reported in this paper has been supported by a postdoctoral fellowship from the Mind Foundation of BC to the first author, the Social Sciences and Humanities Research Council of Canada (SSHRC) grant 36952 and the Natural Sciences and Engineering Research Council of Canada (NSERC) discovery grant 10630 to the second author, and salary awards from the Canadian Institutes of Health Research (CIHR) and the Michael Smith Foundation for Health Research (MSFHR) to the fourth author. We are thankful to Dr. Henk Kiers for providing a Matlab routine for ten Berge and Nevels algorithm used to update **w**'s. We are also grateful to Dr. Liang Wang for providing the memory data and his practical advice. Matlab programs that carried out the computations reported in the paper are available upon request.

References

Abdi, H. (2003). Least squares. In Lewis-Beck, M., Bryman, A., Futing, T. (eds.) *Encyclopedia for Research Methods for the Social Sciences,* (pp.559-561). Thousand Oaks: Sage.

Bühlmann, P. (2002). Bootstraps for time series. *Statistical Science, 17*, 52-72.

de Leeuw, J., Young, F. W., and Takane, Y. (1976). Additive structure in qualitative data: An alternating least squares method with optimal scaling features. *Psychometrika, 41*, 471-503.

Efron, B. (1982). *The Jackknife, the Bootstrap and Other Resampling Plans*. Philadelphia: SIAM.

Friston, K. J. (1994). Functional and effective connectivity in neuroimaging: a synthesis. *Human Brain Mapping, 2*, 56-78.

Friston, K. J., Ashburner, J., Kiebel, S. J., Nichols, T. E., and Penny, W. D. (2007). *Statistical Parametric Mapping: The Analysis of Functional Brain Images*. London: Academic Press.

Gates, K. M., Molenaar, P. C., Hillary, F. G., and Slobounov, S. (2011). Extended unified SEM approach for modeling event-related fMRI data. *Neuroimage, 54*, 1151-1158.

Grady, C.L., Springer, M. V., Hongwanishkul, D., McIntosh, A. R., and Winocur, G. (2006). Age-related changes in brain activity across the adult lifespan. *Journal of Cognitive Neuroscience, 18*, 227-241.

Harville, D. A. (1997). *Matrix Algebra from a Statistician's Perspective*. New York: Springer.

Huettel, S. A., Song, A. W., and McCarthy, G. (2004). *Functional Magnetic Resonance Imaging*. Sunderland, MA: Sinauer Associates.

Hwang, H., and Takane, Y. (2004), Generalized structured component analysis. *Psychometrika, 69*, 81-99.

Hwang, H., DeSarbo, S. W., and Takane, Y. (2007a). Fuzzy clusterwise generalized structured component analysis. *Psychometrika, 72*, 181-198.

Hwang, H., Takane, Y., and Malhotra, N. K. (2007b). Multilevel generalized structured component analysis. *Behaviormetrika, 34*, 95-109.

Hwang, H., Ho, R. M., and Lee, J. (2010). Generalized structured component analysis with latent interactions. *Psychometrika, 75*, 228-242.

Jöreskog, K. G. (1970). A general method for analysis of covariance structures. *Biometrika, 57*, 409-426.

Kiers, H. A. L., and Takane, Y. (1993). Constrained DEDICOM. *Psychometrika, 58*, 339-355.

Kim, J., Zhu, W., Chang, L., Bentler, P. M., and Ernst, T. (2007). Unified structural equation modeling approach for the analysis of multisubject, multivariate functional MRI data. *Human Brain Mapping, 28*, 85-93.

Lahiri, S. N. (2003). *Resampling Methods for Dependent Data*. New York: Springer-Verlag.

Mulaik, S. A. (1972). *The Foundations of Factor Analysis*. New York: McGraw-Hill.

Smith, S. M., Miller, K. L., Salimi-Khorshid, G., Webster, M., Beckmann, C. F., Nichols, T. E., Ramsey, J. D., and Woolrich, M. W. (2010). Network modeling methods for fMRI. *Neuroimage, 54*, 875-891.

Stephan, K. E., Kasper, L., Harrison, L. M., Daunizeau, J. den Ouden, H. E. M., Breakspear, M., and Friston, K. J. (2008). Nonlinear dynamic causal models for fMRI. *Neuroimage, 42*, 649-662.

Takane, Y. (2009). Symbolic computation in generalized structured component analysis (GSCA). *The International Psychometric Society Meeting*, July, 2009, Cambridge, UK.

Takane, Y., Kiers, H. A. L., and de Leeuw, J. (1995). Component analysis with different constraints on different dimensions. *Psychometrika, 60*, 259-280.

ten Berge, J. M. F., and Nevels, K. (1977). A general solution to Mosier's oblique Procrustes problem. *Psychometrika, 42*, 593-600.

Tucker, L. R. (1951). *A method for synthesis of factor analysis studies* (Personnel Research section Report No. 984). Washington, DC: U.S. Department of the Army.

Wang, L., Li, Y., Metzak, P., He, Y., and Woodward, T. S. (2010). Age-related changes in topological patterns of large-scale brain functional networks during memory encoding and recognition. *Neuroimage, 50*, 862-872.

Wold, H. (1973). Nonlinear iterative partial least squares (NIPALS) modeling: Some current devel-

opments. In P. R. Krishnaiah (Ed.), *Multivariate Analysis* (pp. 383-487). New York: Academic Press.

Zhang, G., and Browne, M. W. (2010). Bootstrap standard error estimates in dynamic factor analysis. *Multivariate Behavioral Research, 45*, 453-482.

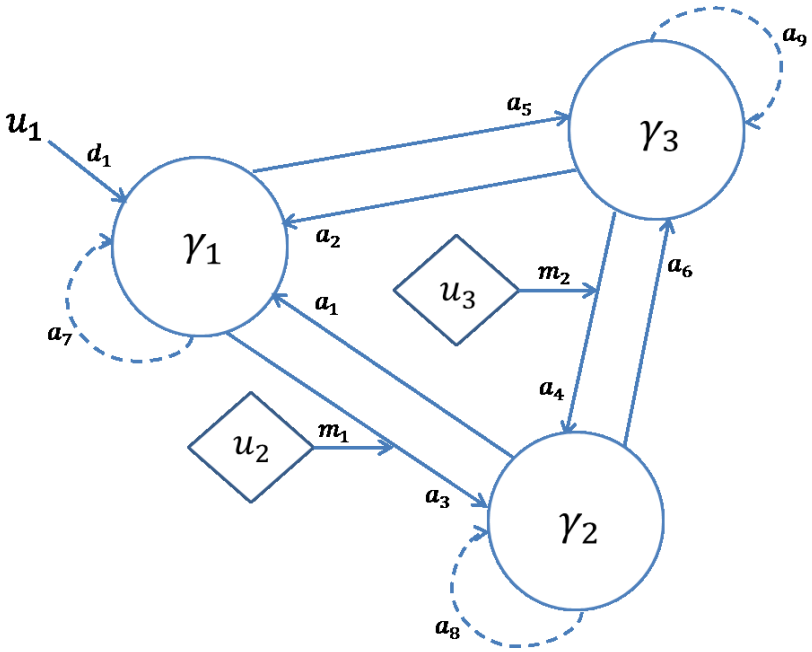

FIGURE 1.
A structural model with three latent variables.

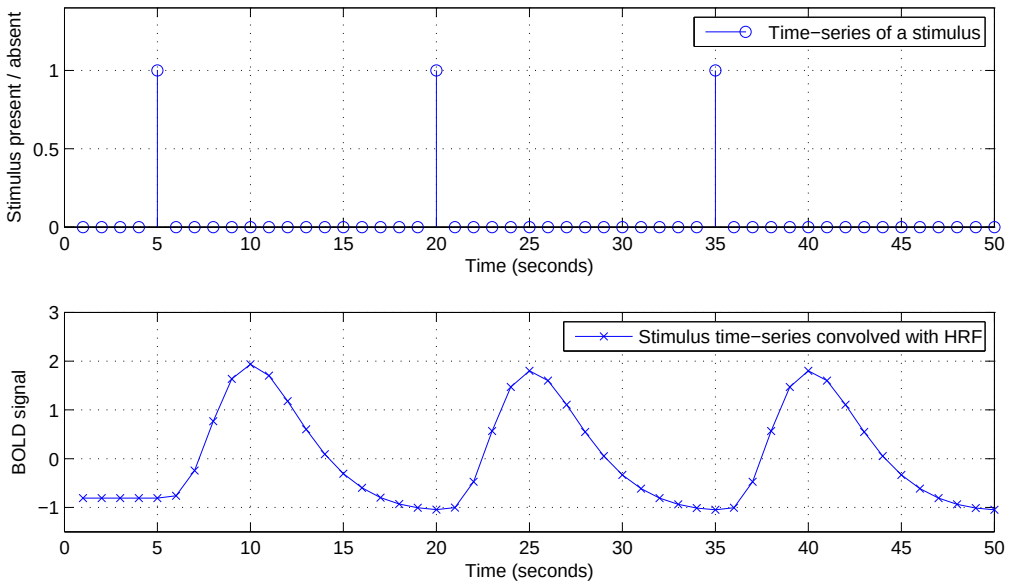

FIGURE 2.
Time series of the first input variable (u_1): A delta function (in the upper panel) and the convoluted input function using HRF (in the bottom).

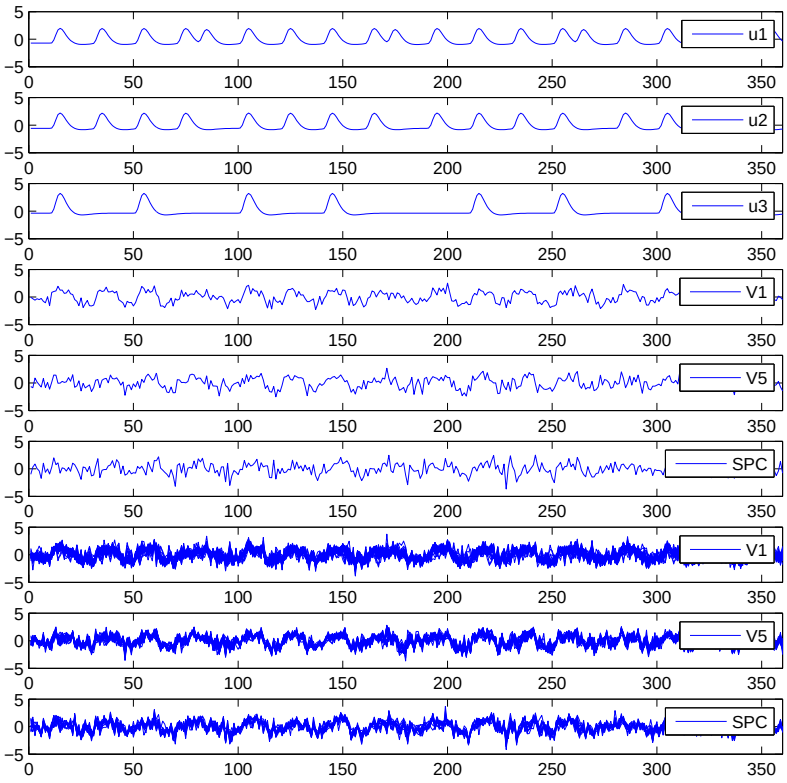

FIGURE 3.
Time series of three experimental inputs and BOLD signals of three ROIs (graphs 4, 5, and 6 depict the BOLD signal of one chosen voxel in the ROI, while graphs 7, 8, and 9 depict the BOLD signals of all voxels in the representative ROI).

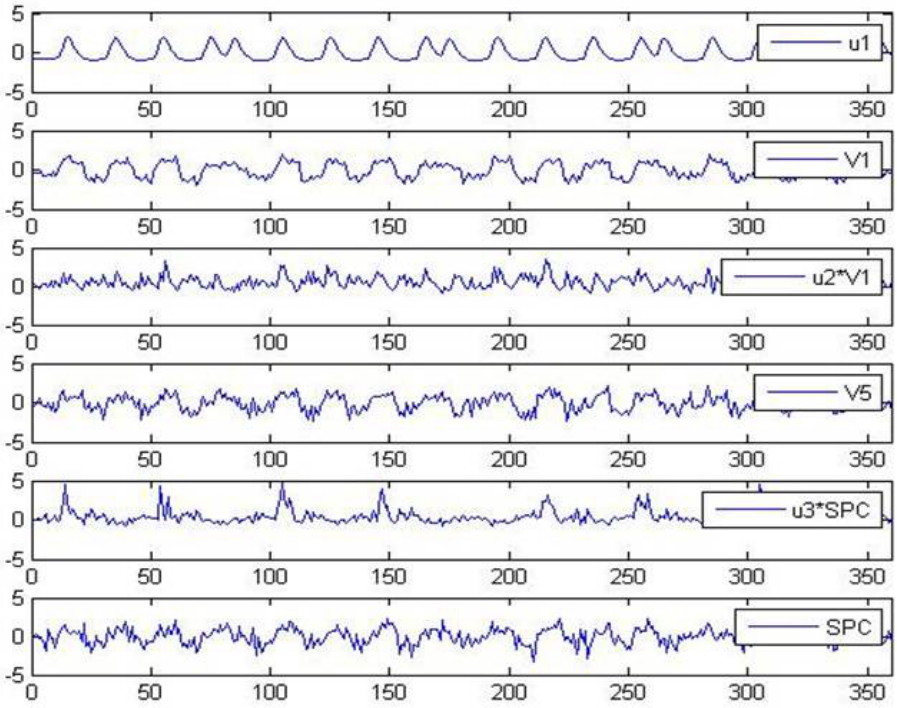

FIGURE 4.
Time series of $\mathbf{u}_1$ and three latent variables (ROIs), and interactions between $\mathbf{u}_2$ and V1, and $\mathbf{u}_3$ and SPC.

TABLE 1.
The mean congruence coefficients with varying error variances and different numbers of time points ($T = 50$, 100, and 200) in study 1 (Standard deviations in parentheses).

	$\tau^2 = 1$		$\tau^2 = 2$	
	Paths	Loadings	Paths	Loadings
$\sigma^2 = 0.3$ (92%)				
$T = 50$	.9316	.9986	.9103	.9987
	(.0433)	(.0006)	(.0470)	(.0006)
$T = 100$	.9692	.9993	.9427	.9993
	(.0141)	(.0003)	(.0204)	(.0003)
$T = 200$	.9834	.9997	.9625	.9997
	(.0074)	(.0001)	(.0132)	(.0002)
$\sigma^2 = 0.5$ (82%)				
$T = 50$	.9263	.9961	.9027	.9964
	(.0350)	(.0016)	(.0469)	(.0016)
$T = 100$	.9605	.9980	.9420	.9981
	(.0182)	(.0009)	(.0282)	(.0007)
$T = 200$	.9808	.9990	.9608	.9990
	(.0097)	(.0004)	(.0152)	(.0005)
$\sigma^2 = 0.7$ (72%)				
$T = 50$	.8969	.9927	.8826	.9924
	(.0605)	(.0034)	(.0628)	(.0035)
$T = 100$	.9543	.9965	.9334	.9965
	(.0241)	(.0015)	(.0304)	(.0017)
$T = 200$	.9755	.9982	.9571	.9982
	(.0123)	(.0008)	(.0168)	(.0008)
$\sigma^2 = 0.9$ (62%)				
$T = 50$	.8703	.9868	.8396	.9876
	(.0791)	(.0064)	(.0851)	(.0051)
$T = 100$	.9376	.9931	.9172	.9936
	(.0354)	(.0032)	(.0417)	(.0027)
$T = 200$	.9689	.9968	.9502	.9968
	(.0154)	(.0014)	(.0236)	(.0013)

TABLE 2.
Power and alpha levels with varying error variances and different numbers of time points ($T = 50$, 100, and 200) in study 2.

	$\tau^2 = 1$		$\tau^2 = 2$	
	Power	Alpha	Power	Alpha
$\sigma^2 = 0.3$ (89%)				
$T = 50$	0.722	0	0.722	0
$T = 100$	0.917	0	0.917	0
$T = 200$	0.972	0.077	0.972	0.077
$\sigma^2 = 0.5$ (78%)				
$T = 50$	0.639	0	0.556	0
$T = 100$	0.806	0	0.806	0
$T = 200$	0.917	0	0.944	0
$\sigma^2 = 0.7$ (67%)				
$T = 50$	0.389	0	0.389	0
$T = 100$	0.778	0	0.694	0
$T = 200$	0.889	0	0.833	0
$\sigma^2 = 0.9$ (59%)				
$T = 50$	0.278	0	0.222	0
$T = 100$	0.556	0	0.556	0
$T = 200$	0.833	0	0.806	0

TABLE 3.
Estimates of path coefficients, their standard errors, and p-values for the attention to visual motion study.

Coeff.	Path	Estimate	S.E.	p-value
a_1	V5 $\rightarrow$ V1	0.347	0.034	0
a_2	SPC $\rightarrow$ V1	0.146	0.037	0
a_3	V1 $\rightarrow$ V5	0.601	0.058	0
a_4	SPC $\rightarrow$ V5	0.307	0.047	0
a_5	V1 $\rightarrow$ SPC	0.335	0.069	0
a_6	V5 $\rightarrow$ SPC	0.404	0.062	0
a_7	V1 $\rightarrow$ V1	0.329	0.034	0
a_8	V5 $\rightarrow$ V5	-0.044	0.055	0.176
a_9	SPC $\rightarrow$ SPC	0.052	0.045	0.136
d_1	V1	0.267	0.032	0
m_1	V1 $\rightarrow$ V5	-0.028	0.043	0.180
m_2	SPC $\rightarrow$ V5	0.018	0.047	0.288

TABLE 4.

Estimates of path coefficients (top), their standard errors (middle), and p-values (bottom) for the memory study. ROIs in rows exert influence on ROIs in columns. The diagonal entries are autoregressive effects of ROIs on themselves. Nonsignificant paths at $\alpha = .05$ are indicated by two asterisks on p-values.

	INS	DCG	HIP	MOG	PCUN	THA	MTG
INS	0.362	-0.288	-0.166	0.022	0.197	0.136	0.050
	(.090)	(.053)	(.060)	(.058)	(.053)	(.055)	(.064)
	0.000	0.000	0.000	0.298**	0.000	0.002	0.222**
DCG	-0.743	0.138	-0.707	-0.096	0.636	0.347	0.235
	(.123)	(.062)	(.089)	(.082)	(.079)	(.104)	(.105)
	0.000	0.006	0.000	0.108**	0.000	0.002	0.014
HIP	-0.389	-0.675	0.120	0.050	0.167	0.406	-0.080
	(.141)	(.077)	(.068)	(.075)	(.096)	(.088)	(.111)
	0.002	0.000	0.066**	0.230**	0.024	0.000	0.232**
MOG	-0.087	-0.144	0.166	0.369	0.300	-0.262	0.650
	(.159)	(.101)	(.109)	(.054)	(.100)	(.077)	(.093)
	0.302**	0.024	0.052**	0.000	0.000	0.002	0.000
PCUN	0.836	0.539	0.249	0.316	0.243	0.266	-0.414
	(.140)	(.068)	(.090)	(.078)	(.075)	(.093)	(.088)
	0.000	0.000	0.004	0.000	0.002	0.000	0.000
THA	0.345	0.280	0.716	-0.089	0.283	0.102	0.527
	(.186)	(.129)	(.109)	(.085)	(.110)	(.083)	(.094)
	0.024	0.014	0.000	0.148**	0.014	0.120**	0.000
MTG	-0.099	0.296	-0.084	0.538	-0.402	0.447	0.066
	(.176)	(.126)	(.132)	(.072)	(.104)	(.079)	(.070)
	0.276**	0.006	0.240**	0.000	0.000	0.000	0.214**